J Mater Sci (2007) 42:9063–9069
DOI 10.1007/s10853-007-1692-9

Effect of chromium addition on microstructure, tensile properties and creep resistance of as-cast Ti-48Al alloy

E. Hamzah · M. Kanniah · M. Harun

Received: 24 November 2006 / Accepted: 13 March 2007 / Published online: 20 July 2007

Abstract The effect of Cr on the microstructure, tensile properties and creep resistance of as-cast Ti–48Al–*x*Cr (x = 0, 2, 4 at.%) alloys were studied. The dependence of the tensile properties and creep resistance of as-cast TiAl on the solid solution strengthening and formation of β phase due to addition of Cr was investigated.

Introduction

TiAl-based alloys are being considered as potential light-weight materials for number of high temperature applications [1, 2]. These alloys consist of high volume fraction of γ phase together with small volume fraction of α_2 phase. One of the major challenges encountered in the development and potential application of two-phase TiAl is how to optimize the mechanical properties. With respect to optimization of the mechanical properties of TiAl, alloying and microstructure control must be considered [3]. Engineering TiAl based alloys should exhibit balanced room temperature ductility, fracture toughness, high temperature strength, creep and oxidation resistance [4]. So far, much effort world-wide has been devoted to studying the effects of thermomechanical processing and alloying in TiAl. The general consensus is, however, that where termomechanical processing results in the improvement of a specific property, it is often at the expense of another [5]. In this regard, alloying chemistry may be used to achieve balanced mechanical properties.

The alloying elements can be classified to two broad groups. The first group of elements is the solid solution strengthening elements or beta stabilizers such as Cr, Mn, V, Nb, Fe, Mo, W, etc., and the second group of elements consists of B, Si and C which provide precipitation or particle strengthening [6]. Among the various alloying elements, Cr is unique in several ways [7]. Firstly, Ti–Al–Cr alloys containing the ternary Laves phase $Ti(Cr,Al)_2$ not only have outstanding oxidation resistance [8], but more importantly, have very similar thermal expansion coefficients to those of γ-alloys. Secondly, theoretical calculations based on the total energy LMTO method have shown that interaction between Cr and Al does not stabilize ω phase formation in the β phase [9, 10]. This makes it possible to ductilise the γ-alloys by compositing the γ phase with a ductile β phase of A2 or B2 structure [7].

This investigation is to study the effect of Cr addition on the microstructure, tensile properties and creep resistance of as-cast TiAl alloy. The microstructure and mechanical properties of as-cast gamma titanium aluminide containing beta phase, Ti–48Al–4Cr are described and a comparison is made with typical two-phase, first generation aluminides exemplified by binary Ti–48Al and solid solution strengthen, Ti–48Al–2Cr. The dependence of the tensile properties and creep resistance of as-cast TiAl on the solid solution strengthening and formation of β phase due to addition of Cr was investigated.

Materials and experimental procedures

The materials investigated in this study have the nominal composition of Ti–48 at.%Al, Ti–48 at.%Al–2 at.%Cr and

E. Hamzah (✉) · M. Kanniah
Faculty of Mechanical Engineering, Universiti Teknologi Malaysia, Skudai, Johor 81310, Malaysia
e-mail: esah@fkm.utm.my

M. Harun
Industrial Technology Division, Malaysian Institute for Nuclear Technology Research, Bangi, Kajang, Selangor 43000, Malaysia

Ti–48 at.%Al–4 at.%Cr. The alloys were produced by IRC University of Birmingham, United Kingdom by plasma melting casting into 2 kg buttons. All the alloys will be referred in atomic percentage hereafter. The samples for metallography analysis were cut using Manho EDM wire cut to 10 mm × 10 mm × 10 mm cube. The samples were ground and polished according to standard procedures. The polished surface was etched using Kroll's reagent (94 ml H_2O + 4 ml HNO_3 + 2 ml HF). The microstructures were examined using Phillips XL40 scanning electron microscope. The grain size and volume fraction is measured using the intercept and point counting methods respectively. The lattice parameters of the alloys were measured by Siemens D 5000 X-ray diffractometer.

Flat samples with dimension, 3 mm × 2 mm with 15 mm gauge length were prepared for the tensile and creep test. Prior to testing, the test pieces were ground along the gauge length in the longitudinal direction to prevent premature crack initiation at surface defects during tension or creep. Instron tensile testing machine was used to perform the tensile testing at room temperature. Constant load tensile creep test was performed at 600–800 °C with initial stresses of 150–180 MPa. The constant load tensile creep test was conducted using Mayes TC 20 High Temperature Creep Testing Machine, consisting three zone temperature furnace and a loading lever arm ratio of 10:1 in air. The test temperatures were maintained constant with a precision of ±1 °C and monitored for 2 h before the test. The temperature was monitored during the creep test by using a thermocouple in contact with the gauge section of the sample. The sample was allowed to soak at test temperature for 1 h before the load was applied. The test was interrupted after 20 h and the samples were left to cool in air to room temperature.

Experimental results

Microstructural characterisation

Ti–48Al and Ti–48Al–2Cr exhibits nearly lamellae microstructure consisting high volume fraction of γ phase (tetragonal, $L1_0$ structure) and a small amount of α_2 phase (hexagonal, $D0_{19}$). Ti–48Al–4Cr too exhibits nearly lamellae microstructure but consist of lamellae, fine γ and β phase. Addition of Cr up to 4 at.%, introduces β phase (bcc structure). The lamellae structure consists of alternating laths of the γ-TiAl and α_2-Ti_3Al phases. Such lamellae structure results from the solid-state phase transformation of the primary disordered α dendrites. The single fine γ regions surrounding the lamellae grains result from the transformation of the aluminum rich interdendritic melt due to incompleteness of the peritectic reactions. The two peritectic reactions, $L + \beta \rightarrow \alpha$ and $L + \alpha \rightarrow \gamma$, is hardly to be completed due to limited diffusion caused by the formation of a solid envelope of the peritectic phase, avoiding the physical contact between the reactants [11]. As far β phase is concerned, even though it is found to exist together with $\alpha(\alpha_2)$ and γ phases in β stabilizer added TiAl, attention has been paid mainly to the role of β phase in the mechanical properties but not to the formation mechanism of the microstructure as well as the phase equilibria among β, α and γ phases. Therefore, the microstructural formation in the alloys under development or study has in most case been interpreted based on the binary phase diagram, since the amount of the additive elements is not large [12]. However, little attempt has been made to establish the phase relationship among the β, α and γ at elevated temperatures [7, 13]. Figure 1a, b and c shows the microstructure of Ti–48Al, Ti–48Al–2Cr, and Ti–48Al–4Cr respectively.

Figure 1 clearly shows that Ti–48Al and Ti–48Al–2Cr exhibits a nearly lamellae microstructure which consists mainly the lamellae grain with a grain size of 500–800 μm and 2–5% of fine gamma grains at the grain boundaries. Even though the lamellae grain size of Ti–48Al and Ti–48Al–2Cr is in a similar range, the volume fraction of γ phase in Ti–48Al–2Cr is significantly higher than in Ti–48Al. The microstructure of Ti–48Al–4Cr consists three phase which are the lamellae (300–600 μm), fine gamma (5–10%) and beta (2–5%) phase. The beta grains are observed to be irregular in shape together with fine γ grains along grain boundaries. Therefore, it is very hard to distinguish between γ and β grains of Ti–48Al–4Cr at low magnifications. SEM image in Fig. 1c clearly reveals the presence of β phase (bright contrast) along lamellae grain boundaries. This type microstructure appears to be commonly observed in β containing TiAl alloy, e.g., Ti–46Al–(1.5–2)Cr–2Mo–0.25Si–0.3B [14, 15], Ti–46.5Al–2Cr–2Nb–0.8Mo–0.2W–0.2Si [16] and Ti-45–10Nb [17]. Table 1 provides the lamellae spacing and grain size of the alloys. Generally, these features are in the similar range.

The composition of all the phases, such as $\alpha_2 + \gamma$ lamellae, γ grains and β phase, were measured using EDX method. The solution of Cr in γ phase increases with addition of Cr (0–4 at.%) in Ti–48Al. The solution of Cr in the β phase of Ti–48Al–4Cr is 11.15 at.%, indicating that Cr is a strong β stabilizer. This results shows that Cr stabilizes β and slightly γ phase. Table 2 shows the compositions of all the phases of the alloys studied.

Table 3 shows the variation of lattice parameter a and c of the γ phase and increment of Cr solution in γ phase with addition of Cr in Ti–48Al. The variation of lattice parameter in the γ phase is complex. The variation of lattice parameter and increment of Cr in γ phase shows the solid solution strengthening of Cr in γ phase.

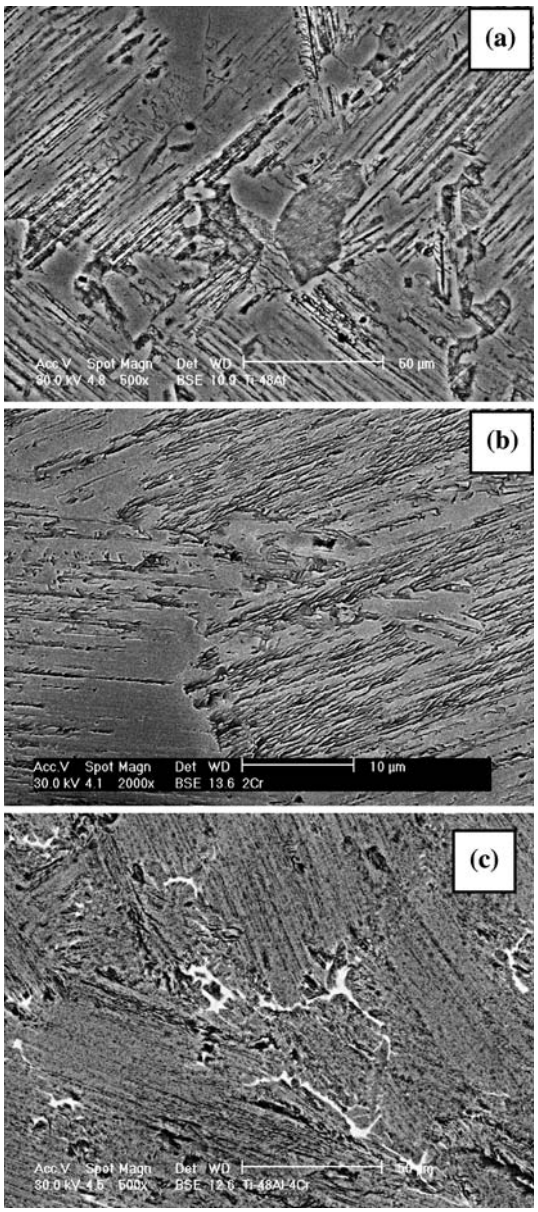

Fig. 1 Microstructure of as-cast (**a**) Ti–48Al, (**b**) Ti–48Al–2Cr and (**c**) Ti–48Al–4Cr

Table 1 Lamellae spacing and grain size of the alloys

Alloys	Lamellae spacing (μm)	Lamellae grain size (μm)
Ti–48Al	1.7	500–800
Ti–48Al–2Cr	1.7	500–800
Ti–48Al–4Cr	1.7	300–800

Room temperature tensile properties

The effect of chromium on fracture strength and ductility of binary, Ti–48Al and ternary Ti–48Al–2Cr and Ti–48Al–4Cr alloys at room temperature are illustrated in Fig. 2a and b respectively. Figure 2a and b shows that fracture strength and ductility significantly increases with Cr addition of up to 2.1 at.%, where the peak strengths and ductility are 540 MPa and 2.15% respectively, and then sharply decrease with further Cr additions of up to 4 at.%. Ti–48Al–2Cr exhibited highest fracture strength and ductility compared to the other two alloys. The increase of fracture strength at room temperature is chiefly attributed by the solid solution strengthening of chromium whereas the increase of ductility is due to contribution of super-dislocation besides the ordinary dislocation in γ phase [6]. The presence of β phase in TiAl decreases the fracture strength and ductility at room temperature. This is because the β phase, with a high content of Cr, is brittle and hard at room temperature. Therefore the sharp decrease in fracture strength and ductility with increasing Cr content is undoubtedly due to the onset of β phase in TiAl. This agrees to the previous research that β reduces tensile strength and ductility [6]. It is reported that the composition where fracture strength starts to decrease after reaching the peak, are the point where β phase starts to form [6].

Table 2 Compositions of $\alpha_2 + \gamma$ lamellae, fine γ and β phase in Ti–Al and Ti–Al–Cr

Alloy	Phase	Ti (at.%)	Al (at.%)	Cr (at.%)
Ti–48Al	$\alpha_2 + \gamma$ lamellae	58.32	41.68	–
	Fine γ	52.88	47.12	–
Ti–48Al–2Cr	$\alpha_2 + \gamma$ lamellae	54.40	43.73	1.87
	Fine γ	53.55	44.19	2.27
Ti–48Al–4Cr	$\alpha_2 + \gamma$ lamellae	52.41	42.86	4.73
	Fine γ	52.56	43.65	3.79
	β	51.62	37.23	11.15

Table 3 Lattice parameter and Cr solution in γ phase of the alloys

Alloys	c (nm)	a (nm)	Cr (at.%)
Ti–48Al	4.049	3.976	–
Ti–48Al–2Cr	24.32	3.971	2.27
Ti–48Al–4Cr	24.32	3.971	3.79

Room temperature fracture

Figure 3a–c shows representative fractographs of Ti–48Al, Ti–48Al–2Cr and Ti–48Al–4Cr following tensile tests at room temperature respectively. Scanning electron microscopy examination indicates a mixed mode of failure for all the alloys. As shown in Fig. 3a, the fracture surface of Ti–48Al exhibits large cleavage facets which are due to

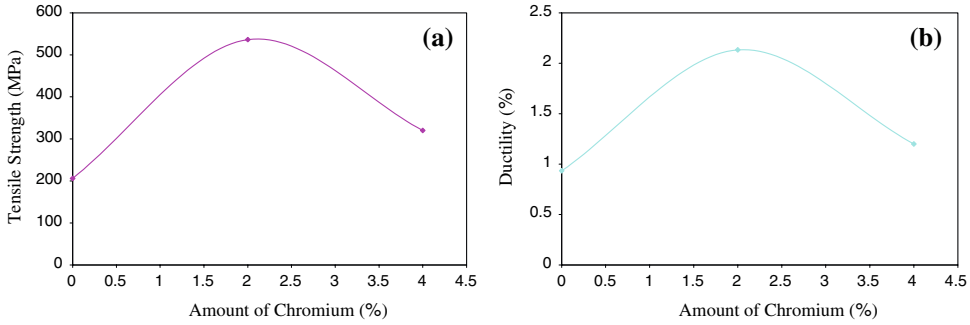

Fig. 2 (**a**) Fracture strength and (**b**) ductility at room temperature as function of Cr content

transgranular fracture across the γ grains. In the lamellae phases, crack propagation appears to progress along the α_2/γ interfaces (interlamellae separation). For Ti–48Al–2Cr, cleavage faceted transgranular fracture of the γ grains is still evident, but a more 'dimple-like' fracture appearance is more generally present (Fig. 3b). This reflects a higher ductility. The fracture surface of Ti–48Al–4Cr (Fig. 3c) are characteristic of flat, featureless facets with a transgranular fracture mode, in which typical elongated cleavage facets corresponding to γ and β phase are observed. This indicates that the β phase in TiAl fractured by a cleavage mode is brittle at room temperature.

Creep resistance

Creep curves of all the three compositions at 600–800 °C with initial stresses 150–180 MPa are illustrated in Fig. 4a–d, with the primary creep strain and secondary creep rate are summarized in Table 4. Figure 4a show creep curves of the alloys at 600 °C with initial stress of 180 MPa. All the three alloys showed steady state creep behaviour. The creep curve of Ti–48Al and Ti–48Al–2Cr is almost identical. The total creep strains accumulated for 20 h, instantaneous creep strain and steady state creep rate of both that alloys is in a similar range. It appears that the solid solution strengthening does not have significant effect on the creep resistance. On the other hand, beta phase contained Ti–48Al–4Cr showed excellent creep resistance compared to Ti–48Al and Ti–48Al–2Cr. The primary creep strain and steady state creep rate is significantly low compared to first generation Ti–48Al and Ti–48Al–2Cr. At 600 °C, the steady state creep rate of Ti–48Al is reduced 69.5% with presence of beta phase (comparison between Ti–48Al and Ti–48Al–4Cr). This figure illustrates the significant effect of beta phase on creep resistance.

Analysis on Fig. 4b shows that the creep response of the alloys at 700 °C with initial stress of 180 MPa is similar as at 600 °C. However, there is slight improvement in creep resistance of Ti–48Al–2Cr compared to Ti–48Al. Ti–48Al–4Cr showed excellent creep resistance. However, the steady state creep rate is only reduced 56% (comparison between Ti–48Al–4Cr and Ti–48Al). It is evident from

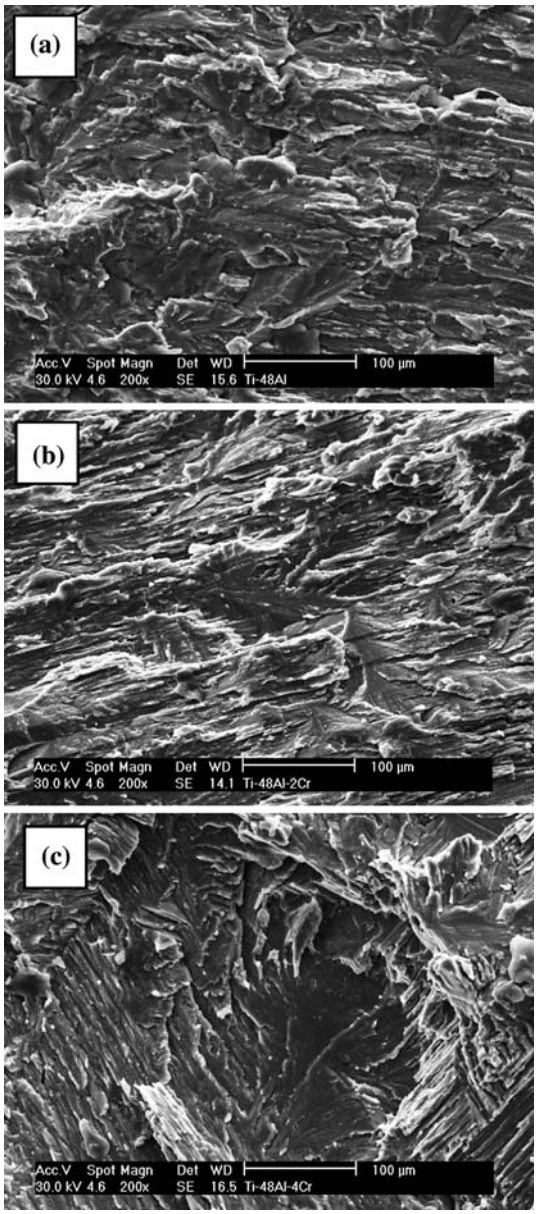

Fig. 3 Fractographs of (**a**) Ti–48Al, (**b**) Ti–48Al–2Cr, (**c**) Ti–48Al–4Cr after tension at room temperature

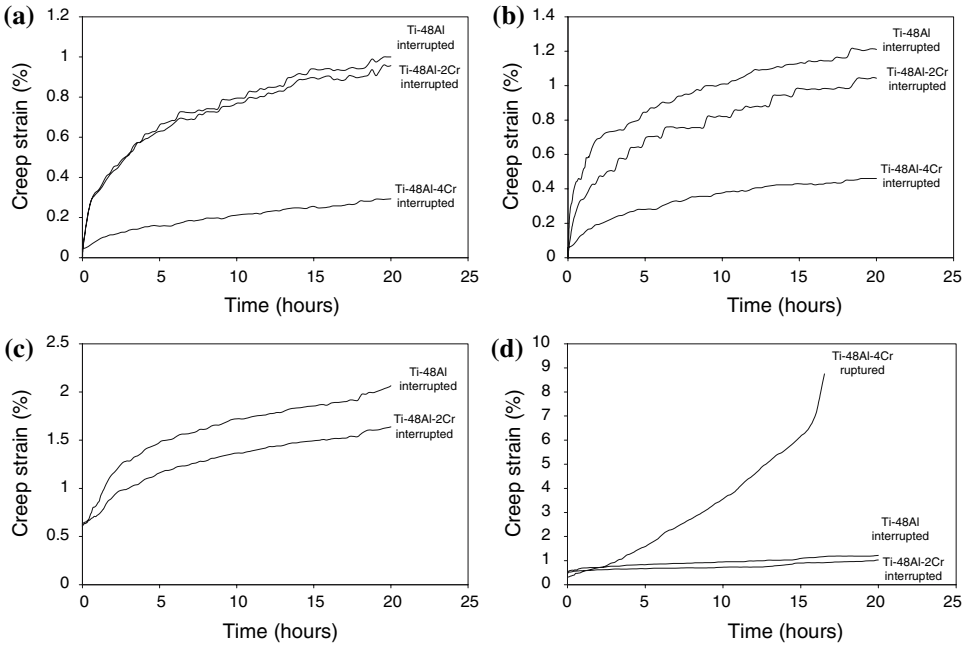

Fig. 4 Typical ε vs. t creep curves of the alloys at (**a**) 600 °C, (**b**) 700 °C, (**c**) 800 °C with initial stress of 180 MPa and (**d**) 800 °C with initial stress of 150 MPa

Table 4 Primary creep strain and secondary creep rate of the alloys

Alloy	Temperature (°C)	Initial stress (MPa)	Primary creep strain (%)	Secondary creep rate (s^{-1})
Ti–48Al	600	180	0.320	2.78×10^{-5}
Ti–48Al–2Cr	600	180	0.310	2.69×10^{-5}
Ti–48Al–4Cr	600	180	0.045	8.49×10^{-6}
Ti–48Al	700	180	0.690	3.23×10^{-5}
Ti–48Al–2Cr	700	180	0.330	2.87×10^{-5}
Ti–48Al–4Cr	700	180	0.060	1.42×10^{-5}
Ti–48Al	800	180	1.340	4.74×10^{-5}
Ti–48Al–2Cr	800	180	0.980	4.06×10^{-5}
Ti–48Al–4Cr	800	180	–	–
Ti–48Al	800	150	0.710	3.13×10^{-5}
Ti–48Al–2Cr	800	150	0.590	2.69×10^{-5}
Ti–48Al–4Cr	800	150	0.680	8.50×10^{-5}

these results that the effect of beta phase on creep resistance depends on the temperature.

Figure 4c shows the creep curves at 800 °C with initial stress of 180 MPa. Ti–48Al and Ti–48Al–2Cr exhibits 0.53% and 0.6% instantaneous creep strain respectively when loaded with initial stress of 180 MPa. Both alloys showed steady state behaviour. However, Ti–48Al–4Cr failed upon loading. It is quite interesting to note that Ti–48Al–4Cr which exhibits low primary creep strains and steady state creep rate compared to Ti–48Al at 600 and 700 °C failed upon loading at 800 °C whereas Ti–48Al and Ti–48Al–2Cr exhibits steady state value until interruption. Therefore a creep test is attempted with initial stress of 150 MPa to study the behaviour of Ti–48Al–4Cr at 800 °C and possible cause for the sudden failure during loading of 180 MPa.

Typical creep curve at 800 °C with initial stress of 150 MPa are shown in Fig. 4d. Ti–48Al and Ti–48Al–2Cr exhibits steady state creep behaviour whereas Ti–48Al–4Cr exhibits minimum creep behaviour. After the initial instantaneous strain, Ti–48Al and Ti–48Al–2Cr undergoes a period of primary creep where the strain rate ($d\varepsilon/dt$) decreases with time to an apparent steady state value that persists for a long period of time until interruption. On the other hand, Ti–48Al–4Cr which exhibits low instantaneous creep strain compared to Ti–48Al and Ti–48Al–2Cr, undergoes a short primary creep and reaches a minimum value before the onset of tertiary creep. This type of creep behaviour is also referred as 'inverse creep' where the creep curve can be divided into two regimes, before and after the minimum creep rate, instead of the common three. Ti–48Al–4Cr sample failed after 16.5 h. Ti–48Al and

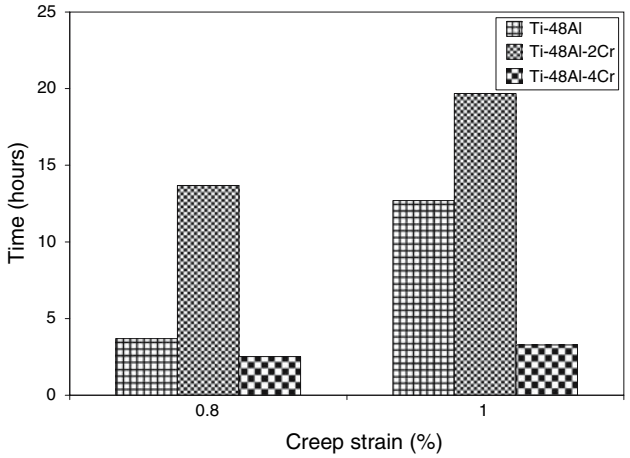

Fig. 5 Time needed to reach 0.8 and 1% of Creep Strain for the Binary and Ternary Alloys

Ti–48Al–2Cr exhibits 0.53% and 0.47% of instantaneous creep strain respectively, whereas Ti–48Al–4Cr exhibits 0.32%. The instantaneous creep strain of Ti–48Al and Ti–48Al–2Cr is in a similar range. Note also that the creep strain of Ti–48Al–2Cr is just slightly less than of Ti–48Al. On the other hand, Ti–48Al–4Cr exhibits greater creep strain before rupture. The period of succeeding accelerating creep rates in the tertiary regime was found to be large and corresponds to roughly 85–90% of the total creep strain to fracture. The time in the tertiary creep regime was about 80–85% of the total time to rupture. The secondary creep rate of Ti–48Al and Ti–48Al–2Cr is almost identical, however, Ti–48Al–4Cr exhibit a greater secondary creep rate. Although, it is common to assume minimum creep rate is equal to steady state creep rate for creep analysis or comparison, however, it does not really accurate. To further compare the alloys, the time necessary to reach 0.8 and 1% creep strains is recorded. Figure 5 shows that Ti–48 Al–2Cr took the longest time to reach 0.8 and 1% creep strains followed by Ti–48Al and Ti–48Al–4Cr respectively. This indicates that solid solution strengthening by chromium in fine γ phase, slightly improves the creep strength. On the other hand, Ti–48Al–4Cr had reached 0.8 and 1% creep strains in a short period which indicates low creep strength. Beta phase deteriorates the creep resistance at high temperature.

Discussion

Role of chromium addition on strengthening mechanisms and microstructural modification

The variation of lattice parameters of γ phase and increment of Cr in γ phase with addition of Cr in Ti–48Al shows the solid solution strengthening of Cr in γ phase. Each alloying element has it own strengthening factor, therefore, it is not necessary that solid solution strengthening by singular alloying element would able to improve all the mechanical properties. It might have strong effect on one and none on the other.

Microstructural features such as lamellae spacing and grain size has significant effect on the mechanical properties of TiAl. These features are usually controlled by heat treatment. However, controlled alloying chemistry, e.g., in this present study; systematic addition of Cr (0–4 at.% Cr) provides a path to study the minor effect of alloying chemistry on microstructural features. The result of microstructural characterization shows that the lamellae spacing and grain size is in a similar range for all the alloys investigated. Therefore, it is concluded that addition of Cr in the present study does not have significant effect on microstructural features. However addition of 4 at.% Cr introduces β phase. Therefore, the variation in mechanical properties between the alloys studied is solely on the solid solution strengthening and β phase.

Effect of chromium addition on tensile and creep properties

The increase of the fracture strength at room temperature with the Cr content is chiefly attributed to the solid-solution strengthening of Cr in γ phase. However, presence of β phase in TiAl does not improve, but deteriorates the fracture strength and ductility at room temperature. It is because the β phase, with a high content of Al and Cr, is brittle at room temperature. Tensile tests show that the Ti–48Al–4Cr has intermediate ductility between Ti–48Al and Ti–48Al–2Cr. Although the fracture strength and ductility of Ti–48Al–4Cr is higher than of Ti–48Al, however it is doubted whether it is due to beta phase or not. The cleavage like fracture surface of Ti–48Al–4Cr after room temperature tension indicates the brittle characteristic of beta phase. Therefore, β phase is undoubtedly detrimental at room temperature due to its extreme brittleness.

Although it had been reported that solid solution strengthening by addition of Cr increases the creep life of TiAl at high stresses [6], however it has no significant effect to the applications. This is due the creep strain exhibited by solid solution strengthening Ti–Al–Cr (Ti–48Al–2Cr) is only slightly lesser than binary Ti–48Al at the intermediate to high temperature. Aerospace and automotive applications not only concerns creep life but creep strain too. Steady state creep rate and the time necessary to reach 1% creep strain of Ti–48Al–2Cr are not significantly improved. On the other hand, β phase becomes very ductile at high temperature due to its open bcc structure [16]. It is evident from the high creep strain exhibited by Ti–48Al–4Cr before

rupture during creep test at 800 °C with initial stress of 150 MPa as shown in Fig. 4d. High creep strain would exceed the tolerance limit of a component and thus prevents the applicability of the alloy. Therefore, β phase is detrimental at both room and high temperature due to its extreme brittle-ductile character. However, this study shows that β phase might be useful at intermediate temperatures. This is due to the excellent creep resistance of Ti–48Al–4Cr compared to Ti–48Al and Ti–48Al–2Cr at temperatures from 600–700 °C. The brittle-ductile character of β phase is suggested to be moderate and therefore have good significant effect on mechanical properties at the intermediate temperatures. From the present study, it is concluded that solid solution strengthening by Cr in γ phase does not have significant effect on creep strength of TiAl and introducing β phase with addition of Cr is found to be detrimental for creep strength with respect to the applications.

Modifications to the alloy chemistry have been attempted in order to maintain a balance between the room temperature ductility and high temperature creep resistance. It is clear that as with all alloys, the high and low temperature properties cannot be generally be optimized simultaneously and the aim of the present program is to assess the optimum alloying routes which allow an acceptable compromise between these properties. It is of course widely accepted limiting factor of the applications of these alloys is their cost and development of cost-effective processing is not been addressed in this paper.

Conclusions

1. As-cast Ti–48Al and Ti–48Al–2Cr exhibited a nearly lamellae microstructure consisting of a high volume fraction of γ phase and a small amount of α_2 phase. Ti–48Al–4Cr too exhibits a nearly lamellae microstructure but the lamellae grain boundaries is occupied by fine γ and body centered cubic (bcc) structured β phase.
2. Addition of Cr stabilizes γ (TiAl) and β phase. The solubility of Cr in γ and β increases with the addition of Cr from 2 at.% to 4 at.%.
3. Ti–48Al–2Cr exhibited the highest fracture strength and ductility followed by Ti–48Al–4Cr and Ti–48Al. The solid solution strengthening by Cr in single γ phase is responsible for this improvement. However, further addition of Cr stabilizes the β phase (Ti–48Al–4Cr) which decreases the tensile properties.
4. All the alloys showed a mixed mode fracture surface after tensile test. Generally, transgranular brittle fracture is more evident due to large cleavage facet corresponding to γ and β phase. Interlamellae separation observed are due to crack along the α_2/γ interface. Slight 'dimple-like' appearance of fracture surface of Ti–48Al–2Cr reflects higher ductility compared to Ti–48Al and Ti–48Al–4Cr.
5. Solid solution strengthening by chromium in γ phase has no significant effect on creep resistance with respect to applications.
6. β phase deteriorates the creep resistance at high temperature. However, presence of β phase has good effect on creep resistance at intermediate temperatures, 600–700 °C.
7. Beta phase is very sensitive to temperature and detrimental for mechanical properties at both room and high temperature.

Acknowledgements The authors would like to thank the Malaysian Ministry of Science, Technology and Innovation (MOSTI) for the research fund under the IRPA program (Project No. 09-02-06-0002 EA-002).

References

1. Yamaguchi M, Inui H (1993) In: Darolia R, Liu CT, Martin PL, Miracle DB, Wagner R (eds) Structural intermetallics. TMS, Warrendale, PA, USA, p 127
2. Kim YW, Dimiduk DM (1991) J Metals 43:40
3. Crofts PD, Bowen P, Jones IP (1996) Scripta Mater 35:1391
4. Marketz WT, Fischer FD, Clemens H (2003) Plasticity 19:281
5. Cheng TT, Wills MR, Jones IP (1999) Intermetallics 7:89
6. Sun FS, Cao CX, Kim SE, Lee YT, Yan MG (2001) Metall Mater Trans A 32:1573
7. Shao G, Tsakiropoulos P (1999) Intermetallics 7:579
8. Brady MP, Smialek JL, Smith J, Humphrey DL (1997) Acta Mater 45:2357
9. Shao G, Tsakiropoulos P, Nguyen-Manh D, Pettifor DG (1997) Phil Mag Lett 76:207
10. Shao G, Passa E, Tsakiropoulos P (1997) In: Nathal MV, Darolia R, Liu CT, Martin PL, Miracle DB, Wagner R, Yamaguchi M (eds) Structural Materials. TMS, Warrendale, PA, USA. p 825
11. Duarte A, Viana F, Henrique M, Santos CM (1999) Mater Res 2:1
12. Takeyama M, Ohmura Y, Kikuchi M, Matsuo T (1998) Intermetallics 6:643
13. Jewett TJ, Ahrens B, Dahms M (1997) Mater Sci Eng A 225:29
14. Schillinger W, Clemens H, Dehm G, Bartels A (2002) Intermetallics 10:459
15. Zhang D, Arzt E, Clemens H (1999) Intermetallics 7:1081
16. Wang JG, Nieh TG (2000) Intermetallics 8:737
17. Zhang WJ, Chen GL, Appel F, Nieh TG, Deevi SC (2001) Mater Sci Eng A 315:250